Inference of lithologic distributions in an alluvial aquifer using airborne transient electromagnetic surveys

Jesse E. Dickinson[1]*, D.R. Pool[1], R.W. Groom[2], and L.J. Davis[2]

*Corresponding author

[1]U.S. Geological Survey, 520 N Park Suite 221 Tucson, Arizona, United States

jdickins@usgs.gov

[2] Petros Eikon Incorporated, Brampton, Ontario, Canada

Abstract

Uncertainty in predicting the potential responses of groundwater systems to hydrologic stresses is related to unknown aquifer extent and properties. Much of this uncertainty is related to sparse well data, especially in alluvial aquifer systems typical of the southwestern United States. Significant lithologic distributions in alluvial aquifers can be inferred from resistivity distributions. An airborne TEM survey was completed along 628 km of flight lines in the Upper San Pedro Basin in southeastern Arizona using the GEOTEM system (Fugro Airborne Surveys, Ottawa, Ontario, Canada) for the purpose of mapping resistivity distributions within the alluvial aquifer. One-dimensional vertical TEM inversions using a constrained Marquardt style under-parameterized inversion indicated a maximum structural resolution of 6 layers underlain by a halfspace to depths of about 200 m meters in conductive areas and greater in resistive areas. A three-dimensional interpolation of resistivity values was developed from the one-dimensional models along flight lines. Results indicated areas of higher electrical resistivity at the basin margins surrounding a region of low electrical resistivity related to thick and relatively impermeable fine-grained deposits of silt and clay in the center of the basin. Interpolated resistivity values compared well with subsurface control data from borehole electrical and lithologic logs indicating that resistivity values can be used to infer basin-wide lithologic distributions in the alluvial aquifer. Areas of uncertain lithology remain at depth and in areas of high salinity. Electrical models were not capable of detecting electrical resistors of coarse-grained alluvial deposits and bedrock underlying electrical conductors of thick silt and clay. High salinity resulted in uncertain lithology in one area.

Introduction

Alluvial basins in the southwestern United States form important aquifers that meet agricultural, industrial, domestic, and municipal water needs. Evaluation of the available water supply, including volumes of water available for extraction and response of the system to hydrologic stress, requires definition of both the spatial aquifer extent and distribution of the hydraulic properties, which are closely related to aquifer lithology. Coarse-grained intervals of sand and gravel are much more permeable and yield larger volumes of water from storage than fine-grained intervals of silt and clay in the semi-confined alluvial aquifers of the area. Silt and clay can form confining beds that locally limit the vertical flow of groundwater between layered aquifers. Distributions of the coarse and fine-grained intervals within the aquifer influence the volumes of water available for withdrawal, groundwater flow paths, rates of groundwater flow, and response of the groundwater system to variations in recharge and withdrawals. However, lithologic distributions are uncertain because of a lack of subsurface information resulting in an inadequate understanding of the groundwater flow system.

Spatial aquifer extent and distribution of coarse- and fine-grained sediments are commonly defined by subsurface materials described by drillers during the installation of water wells. Sparse well data result in uncertainty in both hydraulic property distributions and evaluations of groundwater supply. Many of the data gaps can be filled using geophysical methods (Robinson et al., 2008). In particular, electromagnetic methods can be useful in identifying important variations in lithology because fine-grained alluvial deposits are commonly more electrically conductive than coarse-grained deposits and much more conductive than common non-aquifer rocks such as crystalline rocks (Telford et al., 1976; Pool

and Coes, 1999; Pool and Dickinson, 2007; Fitterman and Stewart, 1986). Electromagnetic and other electrical methods have proven useful for mapping hydrogeologic features in alluvial aquifers and have been used extensively for decades (Zohdy et al., 1974; Smith et al., 2004; Danielsen et al., 2003; Auken et al., 2006; Fitterman and Stewart, 1986; Fitterman, 1987). Electromagnetic surveys have also been used to infer fresh and saline groundwater interfaces (Smith et al., 2004; Fitterman and Deszcz-Pan, 2001), structures that form groundwater basins (Danielsen et al., 2003; Gabriel et al., 2003; Jørgensen et al., 2003; Fitterman et al., 1991; Auken et al., 2003), the presence of perched water (d'Ozouville et al., 2008), locations of possible groundwater recharge zones (Baldridge et al., 2007), and to characterize distributions of fine- and coarse-grained sediments (Rodriguez et al., 2001; Jørgensen et al., 2005; Auken et al., 2003).

The analysis presented here is part of a larger study of the groundwater resources of several alluvial aquifers Arizona, United States conducted by the U.S. Geological Survey (USGS) in cooperation with the Arizona Department of Water Resources (ADWR). The purpose of the portion of the study discussed here is to improve hydrologic conceptual models and to develop computational tools for managing the groundwater resources of the Benson subwatershed of the Upper San Pedro Basin. The approach applies airborne transient electromagnetic (TEM) methods to characterize the hydraulic properties and physical extents of permeable coarse-grained sand and gravel deposits and relatively impermeable intervals of fine-grained silt and clay in the Benson subwatershed (Figure 1).

Interpretation of the TEM data was guided by subsurface control data to develop 3-dimensional (3D) maps of fine- and coarse-grained sediments and hydrologic bedrock that form a framework for parameterizing a groundwater flow model. An approach similar to (Rodriguez et al., 2001) is used to evaluate the use of one-dimensional (1D) electrical models from airborne transient electromagnetic (TEM) data to infer distributions of thick coarse- and fine-grained intervals by comparisons of 1D TEM model resistivity values and resistivity values from electrical logs and important variations in aquifer lithology from drill logs. A combination of inverse modeling of airborne electromagnetic data and geostatistical methods using subsurface control data and resistivity model results are used to (1) evaluate the use of 1D models of airborne TEM data, (2) characterize lithology at three different scales of investigation (point, catchment scale of 15 km^2, and subbasin scale of 2,000 km^2), and (3) develop a 3D distribution of variations in aquifer lithology. The spatial resistivity distributions produced by this simple and direct analysis can be used to infer spatial distributions of aquifer characteristics and groundwater flow paths. The resistivity distributions can be used in the future as an initial data set in a geostatistical approach to improving groundwater flow models of the aquifer in the manner discussed in Robinson and others (2008). The difficulties with interpretation of subsurface electrical conductivity models from the airborne TEM surveys are discussed including (1) the occurrence of conductive overburden in some areas, (2) limited depth of investigation beneath thick conductive intervals, and (3) areas of conductive pre-basin rocks that cannot be separated from fine-grained sediments on the basis of resistivity.

Upper San Pedro study area

The study area is the Benson subwatershed of the Upper San Pedro Basin of southeastern Arizona (Figure 1). The subwatershed occupies an area of about 2,500 km^2 of which about 2,000 km^2 is an alluvial basin that is about 40–50 km wide. The remainder of the subwatershed is primarily the bounding pre-basin rocks that occur in the surrounding mountains and in isolated outcrops near the intermittent San Pedro River that roughly bisects the basin. The land surface, which is predominantly an erosional surface, generally slopes upward from the San Pedro River at an elevation of about 1,000 m to the base of the mountains at an elevation of about 1,500 m. The mountain peaks extend to elevations of more than 2,000 m. Tributaries to the San Pedro River generally flow at right angles to the river, are ephemeral channels, and incised about 10 meters or less below the land surface.

Hydrogeology

The hydrogeology of the San Pedro Basin is typical of many alluvial basins in the southwestern United States (Anderson et al., 1992). Groundwater flows through the basin fill aquifer from recharge areas near the mountains to perennial reaches of the San Pedro River where it discharges to the stream and is transpired by phreatophytes (Pool and Coes, 1999). Rates and directions of groundwater flow are dependent on rates and distributions of recharge, discharge, and distributions of aquifer hydraulic properties. The basin fill aquifer is bounded laterally and at depth by relatively impermeable crystalline rocks of pre-Cambrian and Tertiary age, Paleozoic limestone, Mesozoic sandstone and mudstone, and Tertiary pre-basin sediments (Pool and Coes, 1999). The alluvial basin bounding rocks are not important aquifers with the exception of the Paleozoic limestone, which is locally an important aquifer. The pre-basin fill

rocks have been subjected to Tertiary tectonic deformation including low angle extensional tectonics that resulted in extensive faulting and rotation (Eberly and Stanley, 1978; Shafiqullah et al., 1980; Dickinson, 1991; Scarborough and Peirce, 1978). The basin fill was deposited during and following the waning phases of extensional tectonics. Quaternary erosion resulted in removal of tens of meters or more of basin fill. A narrow stringer of highly permeable stream alluvium is incised into the basin fill along the major stream channels (Hereford, 1993; Pool and Coes, 1999; Cook et al., 2009). The stream alluvium is an important local aquifer that drains the basin fill aquifer, receives streamflow infiltration, and stores water that supports riparian vegetation during periods lacking runoff (Pool and Coes, 1999).

The basin fill aquifer is a sequence of unconsolidated to moderately-well consolidated alluvial sediments of Late-Tertiary and Quaternary age that is greater than 400 m thick in the center of the basin. The basin fill can be divided into lower and upper parts on the basis of geologic logs, drill logs, and geophysical logs (Pool and Coes, 1999). The coarse-grained facies of lower basin fill is commonly described in drill logs as conglomerate or decomposed granite, whereas the coarse-grained facies of upper basin fill is less consolidated and includes many fine-grained interbeds. The fine-grained facies of lower basin fill includes gypsum in a silt and clay or mudstone matrix, and few sand and gravel interbeds. Drill logs indicate that sand and gravel interbeds are common within the fine-grained facies of upper basin fill. Lower basin fill is distinguished from upper basin fill in well logs by greater consolidation, higher density, higher sonic velocity, and fewer fine-grained interbeds. Lower basin fill forms the primary aquifer as the upper basin fill is unsaturated across most of the basin.

The aquifer system is unconfined along the basin margins and confined or semi-confined in the basin center owing to the occurrence of the thick fine-grained facies. In the unconfined portion, the amount of water that can be extracted by pumping is controlled by the hydraulic connection between perforated well intervals and sediments that yield water by a lowered water table and drainage of pore spaces. The amount of extractable water depends on lithology because water drains readily from pore spaces in coarse-grained deposits of sand and gravel, but is retained within the small pore spaces between grains of silt and clay. Groundwater occurs under confined conditions beneath thick sequences of the fine-grained facies where lowering of the water level in wells results in little drainage of pore spaces within the thick fine-grained facies. Semi-confined conditions occur where sufficiently thick fine-grained intervals result in slow drainage of water from pore spaces in response to lowering of the water table. Semi-confined conditions occur at the margins of the intersection of the water table with the fine-grained facies. Definition of distributions of confined, semi-confined, and unconfined groundwater conditions is important for understanding the response of the aquifer system to variations in groundwater withdrawals, volumes of water available for extraction, groundwater flow paths, and rates of groundwater flow.

Subsurface electrical properties

The resistivities of major lithologies in the study area are not well defined by available electrical resistivity surveys. However, the resistivities of lithologic intervals at the two borehole electrical resistivity logs that are available in the study area are similar to resistivity values defined by several electrical and electromagnetic logs at boreholes that encountered similar lithologies in the adjacent Sierra Vista subwatershed (Pool and Coes, 1999). The similarity of

depositional environments and overall lithologic distributions in the two basins suggests that similar resistivity values can be expected from electrical and electromagnetic methods for similar lithologies in the two basins. In addition, the effects of variable water quality on lithologic resistivity are minimal because water is generally of similarly good quality across the two basins.

Galvanic electrical properties of subsurface lithologies in the Sierra Vista Subwatershed are known from borehole geophysical logs and previous electrical and electromagnetic surveys (Pool and Coes, 1999; Pool and Dickinson, 2007; Wynn, 2006; Fleming and Pool, 2002) (Table 1). The most important influence on the resistivity of basin fill is degree of water saturation. Unsaturated sediments can be highly resistive—greater than 100 ohm-m in many cases. Saturated basin fill tends to be much less resistive, ranging from less than 10 ohm-m for clay-rich intervals to more than 50 ohm-m for sand and gravel intervals that include little clay (Figure 3, well D-17-20 31AAB). Older rocks in the area having low permeability include granite, metamorphic, and limestone that are also generally more resistive—greater than 100 ohm-m—than saturated alluvial sediments. However, sedimentary rocks of Mesozoic and older Tertiary age can be indistinguishable from basin fill on the basis of electrical or electromagnetic surveys. Surface geology, borehole geologic logs, or other geophysical information are needed to distinguish basin fill from these older fine-grained sedimentary rocks. Regardless of the inability to distinguish older sediments from basin fill using available data, low resistivity values are indicative of rocks or sediments with low permeability or high salinity that are not suitable for most supply needs. Groundwater quality in the study area is generally good, less than 500 mg/l Total Dissolved Solids (TDS), with the exception of the extreme southwest part of the area

where some marginal water quality, about 1500 mg/l TDS, has been identified (Coes et al., 1999).

Methods

Extent and thickness of significant variations in aquifer lithology were mapped across the alluvial basin using a combination of borehole data, inverse modeling of airborne electromagnetic data, and geostatistical methods. The GEOTEM (Annan and Lockwood, 1991) system of Fugro Airborne Surveys (Ottawa, Ontario, Canada) was used to fly 628 km of airborne TEM surveys (Figure 2). 1D models of resistivity versus depth derived from the airborne TEM data were developed along flight lines. Interpolated 1D models were evaluated at the point scale to borehole resistivity logs, at the catchment scale to 1D models of ground TEM soundings and a geologic section constructed from nearby drill logs, and at the subbasin scale to expected resistivity values of lithologies described by drill logs.

Airborne TEM surveys

The purpose of the airborne TEM survey was to map the aquifer extent within the adjacent non-aquifer crystalline rocks and limestone, and to map thick deposits of fine-grained silt and clay within the coarser grained deposits of sand and gravel. A depth of investigation of 200 to 300 m was need to adequately to map the transmissive portions of the alluvial aquifer on the basis of well data.

GEOTEM was selected as the survey method because of the greater depth of investigation in comparison to helicopter based systems that were available in 2006. The

GEOTEM system consists of a transmitter on an airplane towing a three-coil receiver. The system transmits a periodic (30Hz) electromagnetic field with a waveform having a half-sine current pulse of 4.045 msec. The transmitter is offset from the receiver approximately 132 m horizontally and 39 meters vertically, which theoretically provides better depth resolution than a co-located transmitter and receiver. Originally the data was provided as 5 on-time channels and 15 off-time channels. However, examination of the data set indicated that the transient response with better definition of early and mid-time data would result in improved resistivity models. The original data were therefore reprocessed to provide 20 off-time channels distributed in time to increase early and mid-time samples at the expense of fewer late-time samples which tended to be of insufficient quality.

The GEOTEM survey was flown in April and May, 2006, using a CASA 212 aircraft. The survey included 489 km of north-south lines (25 degrees west of north) parallel to the long axis of the basin and 111 km of east-west cross lines and 2 lines (27km) at 10 degrees east of north (Figure 2). An additional 245 km of lines which trend north-south were flown in the Narrows area which overlaps with the surveys in the northern portion of the Benson Subwatershed. Products of the original GEOTEM data sets included Conductivity Depth Transforms (CDT). The CDTs showed the general distribution of subsurface resistivity, but were not sufficiently accurate to identify and delineate the spatial and vertical distributions of coarse- and fine-grained sediments. Physically-based 1D models of the electromagnetic response of the subsurface that utilize accurate representations of the impulse response of the instrument were therefore pursued.

Control data

The extent and lithology of the basin fill aquifer in the study area is defined by subsurface data of variable quality including altitudes of lithologic picks from drill logs and geophysical logs that are concentrated in developed areas (Figures 1 and 2). Consequently, the aquifer lithology is inadequately defined across much of the basin. The most useful subsurface data are drill logs that include descriptions of materials by a trained geologist and geophysical logs including sonic velocity, electromagnetic, and electrical resistivity (long normal, short normal, and lateral). Geophysical logs are available at only 2 wells (Figures 2, 3 and 4) west of the city of Benson (Figure 1). The primary sources of subsurface data are 1,300 drill logs (Figure 1) that describe general lithologic variations identified during the drilling of water wells.

Borehole electrical logs

Direct-current resistivity logs, using 8- and 64-inch electrode separation, and drill logs including descriptions by a geologist are available for two boreholes compiled by Errol L. Montgomery and Associates, Inc (2006) within the region of TEM surveys (Figure 2). The boreholes, wells D-17-20 31AAB and D-17-20 33DCC, are about two km apart on the west side of the basin and represent only a small range of subsurface conditions found throughout the alluvial basin. A greater range of potential subsurface resistivity values are available from several electric and electromagnetic logs in the Sierra Vista Subwatershed (Pool and Coes, 1999).

Drill logs

Logs that describe subsurface materials identified during the drilling of water wells are available from multiple drillers (Figure 1). These drill logs are of variable quality and detail. An adequate quantity of quality drill logs are available to generally delineate thick intervals of fine- or coarse-grained basin fill in developed areas. In addition, wells are drilled sufficiently deep in isolated areas that the base of the alluvial aquifer can be defined. Aquifer extent and lithology is well defined by drill logs in the upper several hundred meters of the subsurface in developed areas along the basin flanks and the upper 300 m in some areas along the basin axis near the San Pedro River.

Ground-based TEM surveys

Ground TEM surveys were performed at three sites in the study area (Figure 2) for the purpose of evaluating the ability of TEM methods to define subsurface lithology defined by borehole logs and aid in the development of 1D models of airborne TEM data including determining constraints on inversions. The sites were chosen to represent an expected range of subsurface electrical and lithologic conditions. The ground TEM surveys used the Zonge GDP32 system and multiple adjacent transmitter loops (150 x 150 m) at two base frequencies (8 Hz and 16 Hz). Measurements of the vertical component of the magnetic field were collected at the center of each loop and outside each loop at distances of 150m and 225m from loop centers. Measurements outside each loop were completed for improved depth resolution and to evaluate the adequacy of a 1D model. Subsurface control was available from drill logs near ground TEM site 3022 (Figures 2 and 5).

Development of 1D resistivity models of airborne TEM data

One-dimensional resistivity models of airborne TEM data were developed using EMIGMA software (Petros Eikon, 2008), which utilizes accurate representations of the impulse response of the electromagnetic survey instruments. The models were evaluated for adequacy in representing general lithologic and resistivity distributions at three locations where nearby ground TEM surveys and drill log control were available. The ground TEM data were modeled using a Marquardt style under-parameterized inversion (Jia and Groom, 2005 and 2007) through a multi-stage process to confirm data quality, detect significant three-dimensionality in the subsurface, and test the consistency of subsurface structure produced by inversions of center-loop and outside loop measurements. Suitable single models were found to fit both in-loop and outside-loop data at each of the ground TEM sites, which verified the suitability of the 1D models at each site. Multiple outside-loop measurements at each site also allowed for a check of data quality. Any inconsistent outside-loop measurements were removed from the analyzed data set and the remaining measurements were averaged. A joint inversion was done on the center-loop measurement and the averaged outside-loop measurement to produce a general 1D model. The ability of the 1D model to reproduce the airborne TEM data was then evaluated and generalized constraints on inversion of the basin-wide airborne TEM data were developed that produce an approximation of the 1D models of ground TEM data.

The airborne TEM modeling and evaluation process is described using data near site 3022 (Figures 2 and 5). The ground TEM survey was performed using three adjacent transmitter loops on a flat area of alluvial floodplain near the San Pedro River and east of flight line 30080. Measurements of the vertical component of the magnetic field were collected at the center of

each loop and at several outside loop locations at distances of 150m and 225m from each loop center. Processing of the ground TEM data included an evaluation of the data sets and inversion for a single 1D resistivity model that fits all of the inside and outside data sets for all of the transmitter loops. The 8Hz and the 16Hz data displayed very little difference except for greater noise in the late-time 8Hz data. Inversion of the data for loop 1 resulted in model L1, which fits both inside and outside loop data at 150 m north and south of the loop center (Figure 4). Model L1 also generally fits the inside- and outside-loop measurements for the other two loops, with the exception of the southernmost outside-loop station for loop 2, which had a different decay from all the other stations at site 3022. Model L1 consists of 1 m of conducting overburden (1.66 ohm-m) underlain by a 6 ohm-m layer to a depth of 53 m (likely saturated silt and clay) and a 23 ohm-m layer to a depth of 239 m (likely a sandy layer), below which are 3 layers with resistivity values (144 to 222 ohm-m) in the range expected for crystalline rocks or limestone (Figure 5). Model L1 does not quite fit the early-time decay of the center loop data. A lower resistivity value for the top layer improves the fit for the center-loop measurement; however, this is an unexpectedly low resistivity value for unsaturated alluvium. This analysis suggests that the center loop data may not have been collected using the correct system settings; in particular, the pulse width may not have been not measured directly. The inversion was not sensitive to the resistivity of the bottom three layers in Model L1, which indicates that the measurement system and survey geometry were inadequate to define electrical layers underlying the third layer. Thus, the ground TEM data are not adequate to detect the top of resistive bedrock or resistivity of bedrock at site 3022. Improved resolution of the deep resistive

layers may have been possible with measurements at greater offset from loop centers (Davis and Groom, 2009).

Following the analyses at site 3022, a nearby 1 km portion of the 20 off-time channel airborne TEM data near flight line 30080 was examined and 1D resistivity models were developed from Marquardt style inversions along the line. Low resistivity values were used in each starting model on a airborne TEM flight line, as the ground data indicated conductive near-surface materials. At the airborne station that is nearest loop 1 and about 200 m to the west, model L1 fits the airborne TEM data, though the simulated amplitude is slightly lower than observed at early times (Figure 6). The difference at early time may result from uncertainty in the pulse width of the transmitted signal for both the ground and airborne TEM systems. A longer pulse width would increase the response at early times. Similar to the ground data, inversion of the airborne data is also not sensitive to the resistivity of the lower layers.

Comparisons of data at the other two ground TEM sites to the airborne TEM data indicated that a six-layer over a half-space model was sufficient to represent the resistivity layers at each site and was therefore adopted as the model structure for inversion of airborne TEM data. Starting models for inversion of data along flight lines were defined by the best fit model for nearby ground TEM sites. Potential resistivity ranges and constraints in the models were determined on the basis of the results from the suite of models of ground TEM data. The algorithm for inversion of airborne TEM data uses a complex procedure to incorporate system responses and bandwidth and to search exhaustively for best fitting models while removing unnecessary high resistivity structures in the model, which reduces resistivity oscillations with depth. A form of spatial constraints on the variation in the model along the survey line is also

incorporated. At all data locations, inverse models were determined which fit within the estimated noise of the data. Resulting subsurface resistivity structure gradually varies along airborne TEM flight lines suggesting this method of spatial structural determination was reasonably accurate. Resulting models of the airborne data were unable to resolve the resistivity of layers at greater than about 200 m depth.

Interpolation of the 1D resistivity models

Continuous spatial estimates of subsurface resistivity were developed at a resolution of 250 m horizontally by 10 m vertically through two-dimensional (2D) natural neighbor interpolation of the 1D GEOTEM resistivity models at 150 elevation intervals (Figure 8). Data inputs for each interpolation were resistivity values from each 1D model within 10 m thick vertical intervals that span the entire airborne TEM survey from altitudes 1,390 m to -100 m in vertical datum NAVD 88. The resistivity value for each cell was calculated as the arithmetic mean of resistivity values within each 1D 10 m vertical interval that was determined using a natural neighbor search routine. A three-dimensional (3D) resistivity distribution was constructed from a vertical sequence of the 2D grids.

Results of interpolated 1D resistivity models

Interpolated resistivity distribution results are illustrated in Figure 8, which shows the resistivity results at 200 m below land surface for a grid of 250 m spacing. A depth of 200 m was chosen for display because saturated conditions are believed to occur throughout the survey area at that depth. Shallower depths would include unsaturated conditions on the basin

margins. At greater depths, the map would include areas of uncertain resistivity that underlie thick sequences of conductive materials.

Interpolated values between flight lines will be most reliable where resistivity values are laterally continuous across broad areas—i.e., where the subsurface is largely 1D. Interpolated values are less reliable in areas of sharp lateral transitions in resistivity where the subsurface includes 2D or 3D features. Variations that are largely 2D are evident in areas where resistivity values are generally continuous in one orientation but vary along the perpendicular orientation, such as along the margins of conductive materials in the basin center. Likely 3D variations in resistivity occur where "bullseye" patterns occur along flight lines. Twin bulleyes occur along several adjacent flight lines—i.e. lines 30120 and 30130 between lines 38060 and 38050 and lines 30060, 30070, and 30080 south of line 38040—which suggests that the 2D interpolation could benefit from an anisotropic search routine aligned with the major structural orientations. Interpolated resistivity values at sites of subsurface control can be expected to poorly match control points in areas of strong 2D or 3D variations.

Interpolated resistivity values from the 1D models vary within broad and continuous areas of low and high values that generally align along the regional trend of mountain ranges and basins (Figure 8). Resistivity values are mainly restricted to basin fill, but some values are available for bounding bedrock outcrops. Lower values range from less than 10 ohm-m near the central north-south axis of the basin, and larger values greater than 500 ohm-m occur near bedrock outcrops at the basin margins (Figure 8).

Areas of low resistivity values from less than 10 to 30 ohm-m (Figure 8) are common along three major areas. A central area underlies much of the lowest land surface elevations within the central part of the basin, and extends northward areas of shallow bedrock (high resistivity) near line 38040 to another area of high resistivity south of the Narrows. This central area appears to be continuous across the rectangular gap in airborne TEM survey lines over Benson. A southwestern area with low resistivity values surveyed by line 38030 coincides with an area having high salinity (1500 mg/l TDS), which may contribute to lower electrical resistivity in saturated sediments. A western area surveyed by line 38060 is at higher land surface elevations and appears to be discontinuous from the central area.

Areas with larger resistivity values are near small mapped outcrops of Paleozoic sedimentary and limestone rocks that are surrounded by basin fill, south of line 38030 (Figure 8). Resistivity values between values of 30–100 ohm-m occur near and to the east of the small outcrops. Additional areas between values of 30–100 ohm-m occur within a broad area between the large data gap near the cities of Benson and Pomerene and the Dragoon Mountains, and along the Whetstone Mountains. High salinity measured at two wells (1,250 and 651 mg/L) in the southwestern areas may contribute to low resistivity values.

Evaluation of 1D resistivity models

One-dimensional models and interpolated resistivity values were evaluated at three different scales in order to assess the utility of the airborne TEM survey to characterize aquifer lithology. The smallest, the point scale, is evaluated by comparison to borehole resistivity logs at two wells. The catchment scale (15 km^2), is evaluated by comparison of several 1D models of

airborne TEM data in a region that includes several drill logs and a ground TEM survey. Interpolated resistivity values at the subbasin scale (2,000 km^2), are evaluated using geostatistical methods to compare lithologic intervals described by drillers at 166 water wells in a highly developed portion of the basin and qualitatively using drill logs. Because the airborne TEM survey is most useful for rapid characterization at the subbasin or greater scale (Robinson et al., 2008), comparisons to the point and catchment scale were expected to contain only broad similarities in resistivity values and sequences. Comparisons at the subbasin scale, however, were expected to produce interpolated resistivity values that were similar to those of the borehole resistivity logs and from previous studies in the Sierra Vista Subwatershed (Pool and Coes, 1999).

Driller's descriptions were summarized into four lithologic categories for comparison with resistivity—coarse-, medium-, and fine-grained alluvium, and bedrock. These categories were selected because of differences in electrical properties observed in the two borehole electrical logs and in logs from the Sierra Vista Subwatershed. The coarse-grained category is the most resistive and includes mostly cobbles, gravel, and sand. The medium-grained category is moderately resistive and contains sand or gravel with some silt and clay. The fine-grained category is least resistive and contains mostly silt, clay, and mud. The bedrock category broadly includes resistive materials of granite, limestone, and conglomerate, but may include some consolidated mudstones that are expected to be electrically conductive.

Point scale

Interpolated 3D distributions of resistivity were evaluated through comparison to short (8 in) and long (64 in) normal electric logs and lithology described in geologist's and drill logs. A qualitative evaluation included comparison of resistivity from 1D models from the nearest three airborne flight lines and interpolated resistivity with the electric and geologic logs at the two boreholes (Figures 3 and 4), and along geologic section B–B' that includes well D-17-20 DCC and several drill logs (Figure 9).

The 1D resistivity models from three airborne flight lines and interpolated resistivity values near borehole D-17-20 33DCC (Figure 3) all display similar trends and resistivity values, suggesting a largely 1D layered subsurface occurs in the region. Three resistivity layers are apparent from each of the airborne data sets; a thin shallow conductor (10–30 ohm-m) is underlain by a resistive layer (more than 100 ohm-m) above an altitude of approximately 1,175 m; below which each 1D model indicates low resistivity material of 5–20 ohm-m. The low resistivity zone corresponds well with the major lithology of medium to coarse-grained sediment below about 1,160 m. The water table—at an altitude of about 1,110 m—is not evident as a variation in resistivity in the 1D models. The 1D resistivity models from flight line 30040 and 30050 correspond well with the resistivity from borehole electric logs, except for the unsaturated zone which is not expected to be well represented by the borehole logs. The 1D model from flight line 38050 includes the most conductive saturated material of any 1D model (5-10 ohm-m) and the least similarity with the borehole electric logs. Interpolated resistivity values at the borehole are similar to borehole resistivity values below the water table and are similar to the resistivity of the saturated materials at borehole D-17-20 33DCC.

The electric logs and 1D models from airborne data at borehole D-17-20 17AAB (Figure 4) indicate greater spatial variability in subsurface resistivity values than at borehole D-17-20 33DCC (Figure 3). The 8 and 64 inch electric logs display similar resistivity trends throughout the borehole. Resistive zones (> 50 ohm-m) occur above an altitude of about 1,160 m and below about 1,000 m. More conductive material of 5–25 ohm-m occur in the intervening zone. Similar to borehole D-17-20 33DCC, the water table is not evident as a resistivity variation in the electric logs. Higher resistivity values of the 64-inch electric log are likely more representative of the subsurface materials than values from the 8-inch electric log. The lithologic log at borehole D-17-20 17AAB displays layers that mimic the electric intervals in the electric logs; a fine-grained and electrically conductive zone between altitudes of about 1,155 and 1,085 m is bounded above and below by more coarse-grained and electrically resistive zones.

The 1D resistivity models from three airborne flight lines near borehole D-17-20 17AAB indicate that the borehole is in a region of high spatial variability. The model of data from flight line 30030 resulted in a much more resistive subsurface than the models of data from lines 300040 and 38050. Flight line 30030 is furthest from the borehole and the TEM data are likely influenced by nearby resistive bedrock (Figure 2). As a result, the 1D model from flight line 30030 is not likely representative of the subsurface at the borehole. The 1D model of data from flight line 30040 suggests a slightly more resistive saturated zone than the model of data from line 38050; about 20 and 5 ohm-m, respectively below an altitude of about 1,160 m. However, both models indicate a conductive layer occurs below an altitude of about 1,200 m. Models from neither flight line detected the lowermost resistive zone that was present in the electric and lithologic logs, indicating a depth of investigation of less than 300 m. Interpolated resistivity

values at borehole D-17-20 17AAB do not represent the electric and lithologic logs well as the transition from shallow resistive material to more conductive material at depth is much more gradual than is indicated by the subsurface control data. Much of the deviation from observed conditions results from the 1D model of data from flight line 30030. Comparison of the interpolated resistivity values with observed data at this region of high spatial variability suggests that a distance weighted interpolation algorithm may result in more accurate interpolation.

Catchment scale

The 1D models were evaluated at the catchment scale for adequacy in representing the generally expected resistivity distributions where nearby ground TEM surveys and drill log control were available. The evaluation process is described using subsurface data from several well logs along geologic section A–A', which is approximately 600 m north of site 3022 (Figures 2 and 5). Models of airborne TEM data are available from flight lines 30070, 30080, and 38040, which cross the geologic section. Similar subsurface conditions are expected to also occur in the region of the line 30080 near site 3022. Drill log data along the section indicate three distinct lithologic and resistivity layers underlying the water table (3–20 m depth). Low resistivity materials of silt and clay (<20 ohm-m) near the surface are underlain by intermediate resistivity materials of predominantly or sand and gravel conglomerate (20–70 ohm-m) at depths 80–140 m and bedrock (>100 ohm–m) at greater than 100 m depth. Lithologic variations along the section include an overlying thin layer (5–20m) of recent sand and gravel alluvium near the San Pedro River, and greater depth to bedrock at the southeast margin of the section. Variations in groundwater salinity are not expected to cause variations in electrical properties in the area of

the section, and salinity is generally low on the basis of several well samples (USGS National Water Information System, http://waterdata.usgs.gov/nwis, accessed December 2009).

Model L1 at site 3022 roughly matches the resistivity layers expected on the basis of the nearby drill logs (Figure 5). The shallow conductor (1 ohm-m) is less resistive than expected for this lithology (about 10 ohm-m), but could result from the accumulation of salts in clayey soils above a water table that is within a few meters of the surface. Shallow sampling of the unsaturated zone for water content and salinity could verify or eliminate the possibility of the low resistivity values. Low salinity would support the possibility that large early-time amplitude in the ground TEM data result from a poorly-defined transmitter pulse width. Model L1 required a more resistive layer (23 ohm-m) of undetermined thickness at a depth of 53 m beneath the shallow conductive layers, which generally matches the drill log data. However, the 1D model alone has insufficient information to map the thickness of the intermediate resistive layer of sand and gravel. The well logs indicate bedrock occurs at a depth of about 100 m or more, but models of the ground EM data were not sensitive to the resistivity or thickness of this layer. The lack of resistive bedrock detection by the ground TEM survey indicates that the depth of investigation at site 3022 was less than 100 m and likely limited by the shallow conductor.

Inversions of the airborne TEM data in the vicinity of geologic section A–A' and site 3022 resulted in subsurface resistivity models that were similar to those expected from the well data. The similarity of 1D models of data from flight lines 30070, 30080, and 38040 indicates that the inversion process was well suited for the data (Figure 5). The upper 50 m are dominated by low resistivity layers of 10 ohm-m or less , but each model also included a single more resistive layer

(23–100 ohm-m) of about 30 m thickness. Variations in resistivity in the upper 50 m likely result from variability of the lithology and resistivity of near-surface alluvial deposits, and of the thickness of the unsaturated zone across the area. Resistive sand and gravel near the surface ranges in thickness from 0 to 40 m at the wells. Depths to water range from 1 m to 20 m. The upper 50 m was generally underlain by a low resistivity layer (less than 10 ohm) in the 1D resistivity models that corresponds to the upper silt and clay (100–150 m thick) interval identified at each well along the geologic section. The 1D models were not sensitive to the resistivity and thickness of deeper layers; therefore, the intermediate sand and gravel interval underlying the upper silt and clay interval and deeper bedrock were not resolvable by the airborne survey in this area. Regions of thick silt and clay, such as near site 3022, likely resulted in the shallowest depth of investigation in the study area. In areas outside of the thick silt and clay deeper layers could be resolved to depths of as much as 200 m.

Subbasin scale

The interpolated resistivity values from the 1D models were evaluated at the subbasin scale by comparisons with expected resistivity values of lithologies described in drill logs. Lithology was categorized as fine-grained, medium-grained, coarse-grained, or bedrock. The comparison included 166 drill logs (Figure 8) west of the city of Benson that penetrated fine-grained facies at the basin center and hydrologic bedrock near the Whetstone Mountains. Interpolated resistivities were similar to values measured at boreholes D-17-20 31AAB and D-17-20 33DCC and within the Sierra Vista subwatershed (Figure 10 and Table 1). Mean resistivity values for each 10 m altitude range of the interpolated resistivities for the fine-grained category averaged 8 ohm-m. The standard deviation is low (maximum of 11 ohm-m between 1090 m and

1100 m), indicating that interpolated resistivity values were consistently low at fine textures. Mean values were similar for the medium-grained category (14 ohm-m), but the standard deviation of 30 ohm-m was greater between altitudes 970 to 990 m, which suggests that inferred lithology may be more uncertain at these altitudes. For the coarse-grained category, the mean value was 65 ohm-m, and the mean values varied up to 50 ohm-m between per 10 m altitude range. Such widely-ranged values may be due to inaccurate drill logs, and that the resistivity models do not include sufficient heterogeneity to represent highly-varying sediment textures. The mean value for bedrock is 21 ohm-m, and ranges from 10–100 ohm-m among the 10 m altitude ranges. The variability may due to fine-grained mudstones, limestone, and granite being commonly described as bedrock in drill logs.

Inferred lithology based on electrical resistivity and drill logs

Qualitative and quantitative correspondence of the inverse electrical resistivity models to borehole electrical logs and drill logs indicate useful relations between lithology and modeled electrical resistivity distributions. To generally discuss the lithologic interpretation of resistivity distributions, only the mapped distribution at a depth of 200 m below land surface (Figure 8) and along geologic section B–B’ (Figure 9) are presented. The distribution of resistivity at 200 m depth generally reflects the distribution that would be expected for basin fill sediments deposited in an alluvial basin under conditions of closed or restricted drainage. The most conductive material (20 ohm-m or less) is a fine-grained facies dominated by silt and clay in the basin center. The fine-grained facies is surrounded by a more resistive facies (20–100 ohm-m) that is dominated by sand and gravel deposits. Bedrock may be represented by

resistivity values of 100 ohm-m or greater along the basin margins and near the San Pedro River at airborne TEM line 38040. The only known area of poor water quality that would mask the lithologic effect on resistivity occurs at the southwestern extent of flight lines 38030, 38010, and 38020.

The depth distribution of resistivity values is illustrated along generalized geologic section B–B' (Figure 9). The section crosses the central part of the basin and includes most of the major electrical and lithologic features in the alluvial basin (Figure 8). Areas of high resistivity on the section margins grade to low values in the basin center in both the saturated and unsaturated zones. Resistivity values less than 10 ohm-m dominate most of the central part of the section. Areas of intermediate resistivity, 20–30 ohm-m, closely flank the region of low resistivity and overlie the low values east of the san Pedro River. Resistivity values in the saturated zone compare well with interpolated values at borehole D-17-30 33DCC where both the borehole and interpolated resistivity data sets indicate 20–30 ohm m material. Resistivity values shown at depth on the section, 300 m on the basin margins and 200 m in the basin center, are uncertain because the top and resistivity of the lowest layers are not well constrained by the 1D models, especially in the area of thick low resistivity materials.

Lithologic distributions are inferred using a combination of drill logs in developed areas and resistivity distributions in undeveloped areas (Figure 9). Crystalline bedrock and limestone occur on the basin margins. A thick sequence of basin fill, more than 300 m, including a thick interval of silt and clay, as much as 200 m, is underlain by sand and gravel in the deepest part of the basin. Data from drill logs define the top of the fine-grained materials in the basin center.

However, the fine-grained materials extend beyond the area of well logs on the basis of a zone of resistivity of 10 ohm-m or less. Low resistivity values generally define only the top of the fine-grained facies because resistive layers beneath thick intervals of silt and clay could not be resolved by the 1D models. The fine-grained facies is bounded at the top and lateral margins by an interval of 10–30 ohm-m material that likely represents medium-grained sediments and a gradational facies from the fine- to the surrounding coarse-grained facies of basin fill. A significant wedge of medium-grained basin fill is defined by drill log data east of the San Pedro River and appears to be well mapped by a wedge of 10–30 ohm-m resistivity. At borehole D-17-30 33DCC, a zone of 10–20 ohm-m that occurs at depths of about 170 to 210 m in the electric log likely represents the margins of the fine-grained facies that is evident as a thick interval of 10 ohm-m or less immediately east of the well.

Uncertain lithology derived from resistivity distributions occurs beneath thick intervals of conductive materials, in areas of high salinity groundwater, and where multiple lithologies have similar resistivity values. Coarse-grained sediments that underlie conductive sediments at the basin center are not resolved by the 1D resistivity models. Thick intervals of conductive sediments in the deepest parts of the alluvial basin prevent detection of underlying coarse-grained sediments, which are hydrologically important and is heavily exploited for groundwater supply in the study area. The extent and thickness of the coarse-grained interval remain uncertain except were the interval is defined by many drill logs at the center of the basin. Low resistivity values (<10 ohm-m) coincide with high salinity in the southwest portion of the study area (Figure 8), although some drill logs indicate fine-grained sediments in that area. At the western portion between the Whetstone and Rincon Mountains (Figure 8), resistivity values

less than 20 ohm-m meters appear to be separate from the thick fine-grained sequence at the basin center, and may be consolidated pre-basin mudstones.

The extents of fine-, medium-, and coarse-grained facies identified by the airborne TEM survey are expected to have strong influence on groundwater flow in the aquifer system (Figure 9). This allows for delineation of semi-confined groundwater conditions in areas underlying the fine-grained sediments, and unconfined conditions where fine-grained sediments are less extensive. The extents also provide spatial constraints on hydraulic parameters that govern groundwater flow rates and the amount of stored groundwater. These interpretations are valuable for other components of the groundwater resources study of the San Pedro Basin, and may prove useful for constructing groundwater flow models for analyzing groundwater resources.

Conclusions

One-dimensional models of airborne TEM surveys can be used to map important lithologic distributions and infer aquifer hydraulic properties where drill log data are scarce or of uncertain quality. The ability of the 1D models to map aquifer lithology was evaluated at three scales through comparison with borehole resistivity logs at the point scale, lithologic descriptions from several drill logs at the catchment scale, and lithologic descriptions from many drill logs at the subbasin scale. The analysis is completed for an airborne TEM survey of the alluvial aquifer in the Benson Subwatershed of the Upper San Pedro Basin of southeastern Arizona in order to improve hydrogeologic framework models, understanding of the groundwater flow system, and construction of groundwater flow models.

Subsurface resistivity values for various alluvial and bedrock lithologies are defined by electrical resistivity logs in the study area and electric and electromagnetic logs and surveys in the adjacent Sierra Vista Subwatershed, which has alluvial units that were deposited in similar environments. One-dimensional (1D) models of ground-based TEM soundings at three sites were used to determine starting models and constraints for inversion of 1D models of the airborne TEM data. Inversions of the ground TEM data were performed with a constrained Marquardt style under-parameterization (Jia and Groom, 2005 and 2007). Inversions of the ground TEM data were performed using a multi-stage process to confirm data quality, detect significant three-dimensionality in the subsurface, and test the consistency of subsurface structure produced by inversions of center-loop and multiple outside-loop measurements. A six-layer over a half-space model was assumed for the inversions of the airborne TEM data on the basis of the subsurface resistivity layers in the models of the ground TEM data.

At the point-scale comparisons, electrical and geologic properties from two borehole resistivity logs were closely related to 1D resistivity models of nearby airborne TEM data. The two resistivity logs and 1D models identified an upper sequence of highly-variable resistivity values identified as interbedded sand, gravel, and clay. Below the upper sequence, the resistivity logs and 1D models range between 5–20 ohm-m within a silt and clay sequence. Underlying the silt and clay to the bottom of the boreholes, the resistivity logs and 1D models increase to several hundred ohm-m and are highly variable within sand and gravel layers. These sequences matched distinct resistivity and lithologic layers identified by geophysical logs in the adjacent Sierra Vista Subwatershed, suggesting that these sequences are laterally continuous within both the Benson and Sierra Vista Subwatersheds in the Upper San Pedro Basin.

At the catchment scale, 1D models of the airborne TEM data included a sequence of layers that were expected from lithologic descriptions from several drill logs. Drill logs indicated a thick upper layer of silt and clay and an intermediate layer of sand and gravel that overlies bedrock. The upper 50 m of the 1D models were dominated by low resistivity layers of 10 ohm-m or less. Each model also included a single more resistive layer (23–100 ohm-m) of about 30 m thickness that may be attributed to more resistive sand and gravel not included in drill logs and unsaturated sediments. The intermediate sand and gravel and bedrock were not resolved by the 1D models.

Comparisons of the interpolated 3D distribution of resistivity to lithologic descriptions at drill logs at the subbasin scale indicated that resistivities of lithologies in the study area are similar to the values measured at the boreholes D-17-20 31AAB and D-17-20 33DCC and in the

Sierra Vista Subwatershed. The mean interpolated resistivity values were 8 ohm-m for fine-grained sediments, 14 ohm-m for medium-grained sediments, 65 ohm-m for coarse-grained sediments, and 21 ohm-m for bedrock.

Significant resistivity zones mapped from 1D models of airborne TEM surveys correspond with hydrologically-significant lithologic zones. Stratigraphic sequences indicated in borehole logs and the 1D resistivity models are indicated by the resistivity models throughout the study area. Within basin fill sediments, this includes fine-grained zones of silt and clay of low permeability, medium-grained zones of sand-silt gravel and clay, and coarse-grained zones of sand and gravel and conglomerate. Lithologic zones of crystalline and limestone bedrock underlie the basin fill sediments. New spatial extent and thickness of the lithologic zones obtained from this study may be included in numerical groundwater flow models to reduce the uncertainty of water resources projections.

Acknowledgements

Funding for the GEOTEM survey, electrical modeling, and data analysis was provided by the Arizona Department of Water Resources (ADWR) and the U.S. Geological Survey Arizona Water Science Center. Important data sources included well logs obtained from the GWSI well database from the Arizona Department of Water Resources, and geophysical logs obtained from Daniel Weber of Montgomery and Associates, Inc. in Tucson, Arizona. Jamie Macy and James Callegary of the USGS collected ground TEM measurements. The authors thank Ty P. A. Ferré of The University of Arizona, Frank Corkhill of ADWR, and three anonymous reviewers for

their comments. The use of brand names does not constitute product endorsement by the U.S. Geological Survey.

LIST OF FIGURES

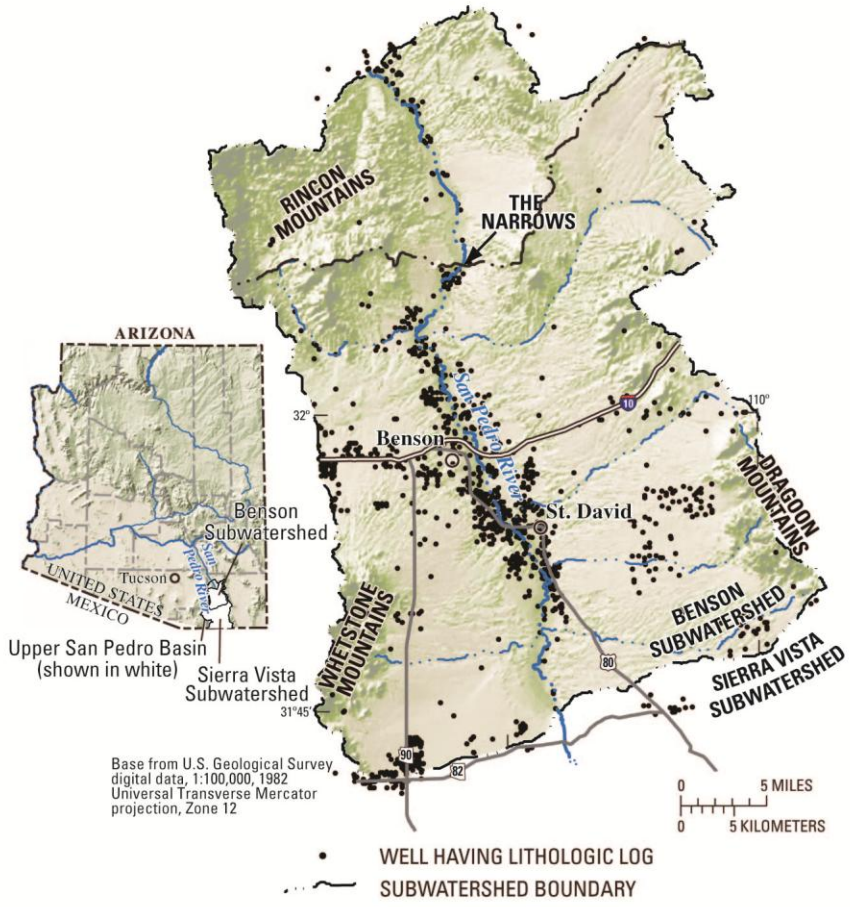

Figure 1 Benson Subwatershed of the Upper San Pedro Basin study area in Arizona, United States. Sparse wells having lithologic logs result in uncertain lithology and aquifer properties.

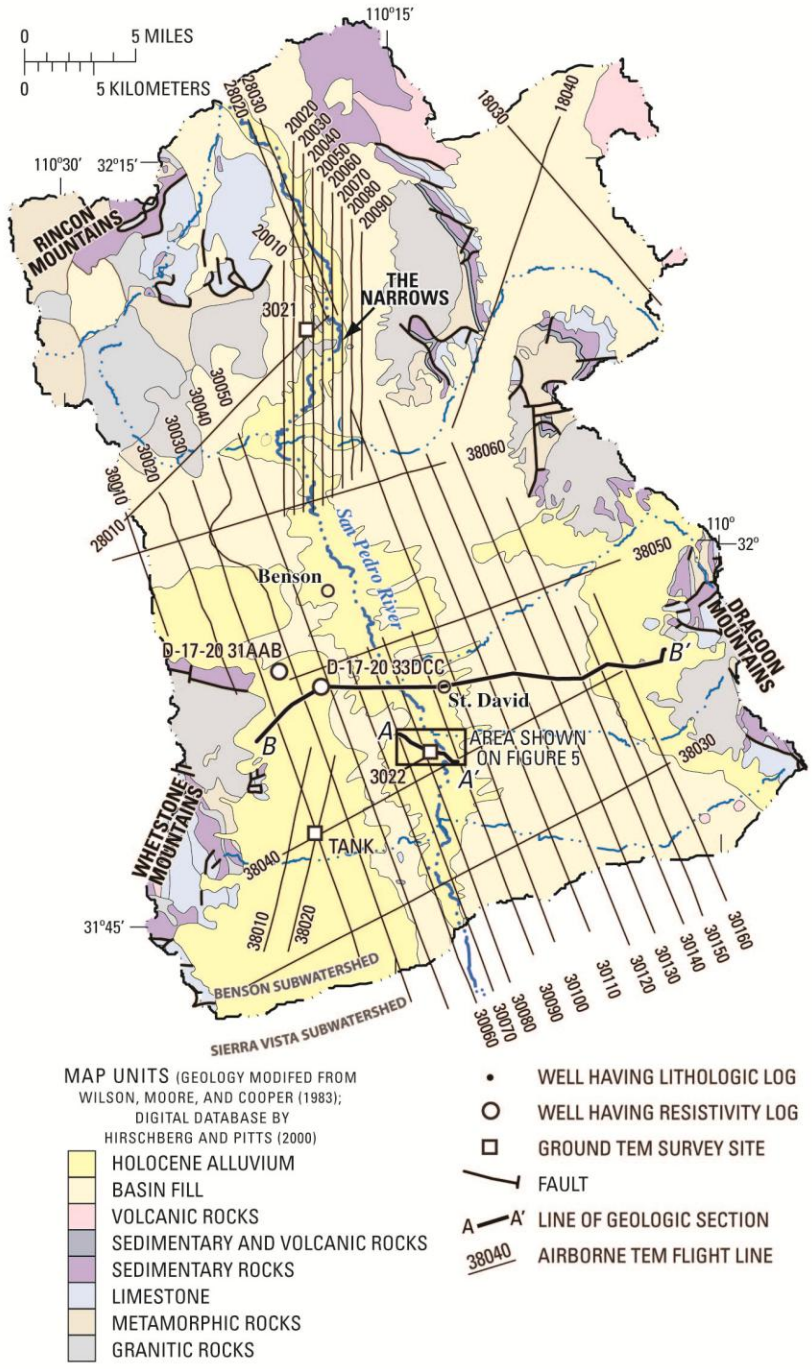

Figure 2 Generalized geology, airborne TEM flight lines, ground TEM survey sites, and boreholes having resistivity logs in the Benson Subwatershed. The late Miocene to Quaternary alluvial basin fill aquifer is bound by uplifted fault blocks of pre-Tertiary crystalline and sedimentary rocks. Section A–A', shown on figure 5, traverses through ground TEM site 3022 and section B–B', shown on figure 8, traverses west to east through areas of dense airborne TEM flight lines and boreholes with drill logs.

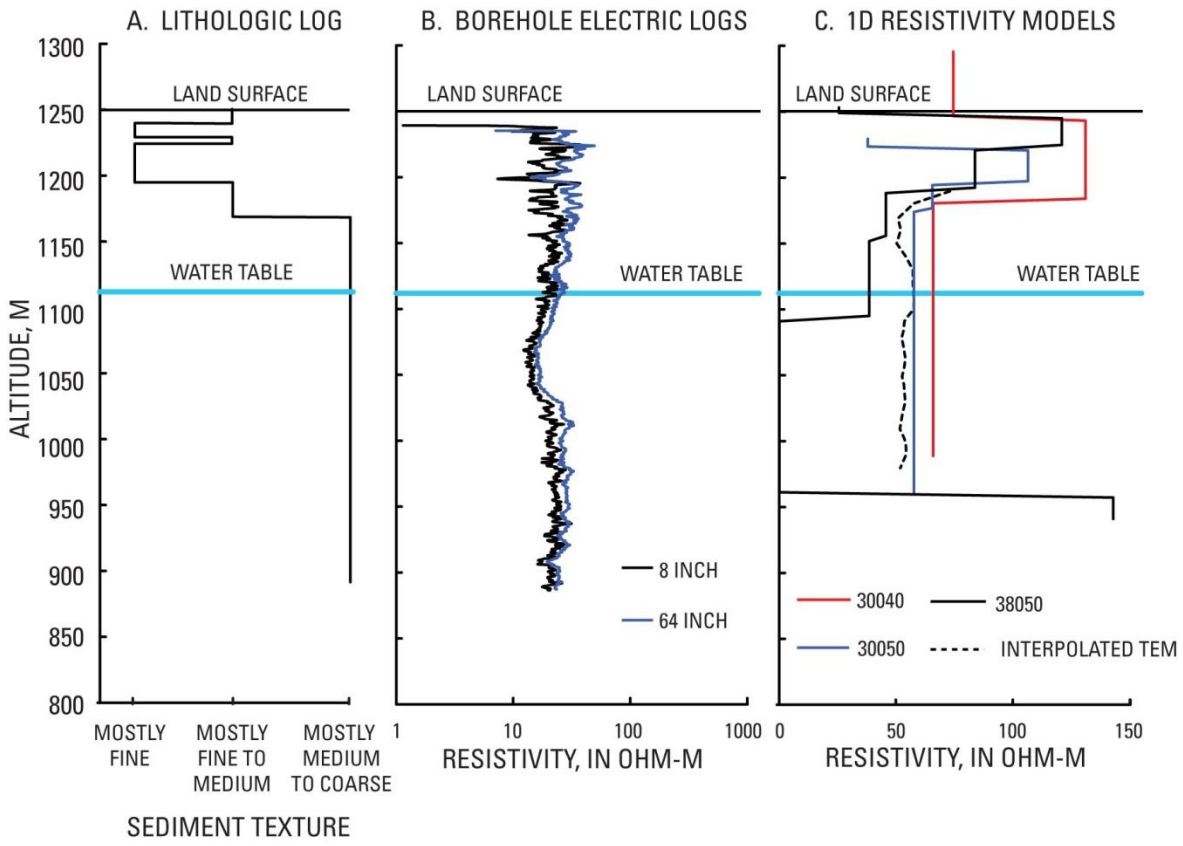

Figure 3 Comparison between resistivity logs, interpolated output from 1D resistivity models along nearby GEOTEM flight lines, and sediment texture from lithologic logs at well D-17-30 33DCC.

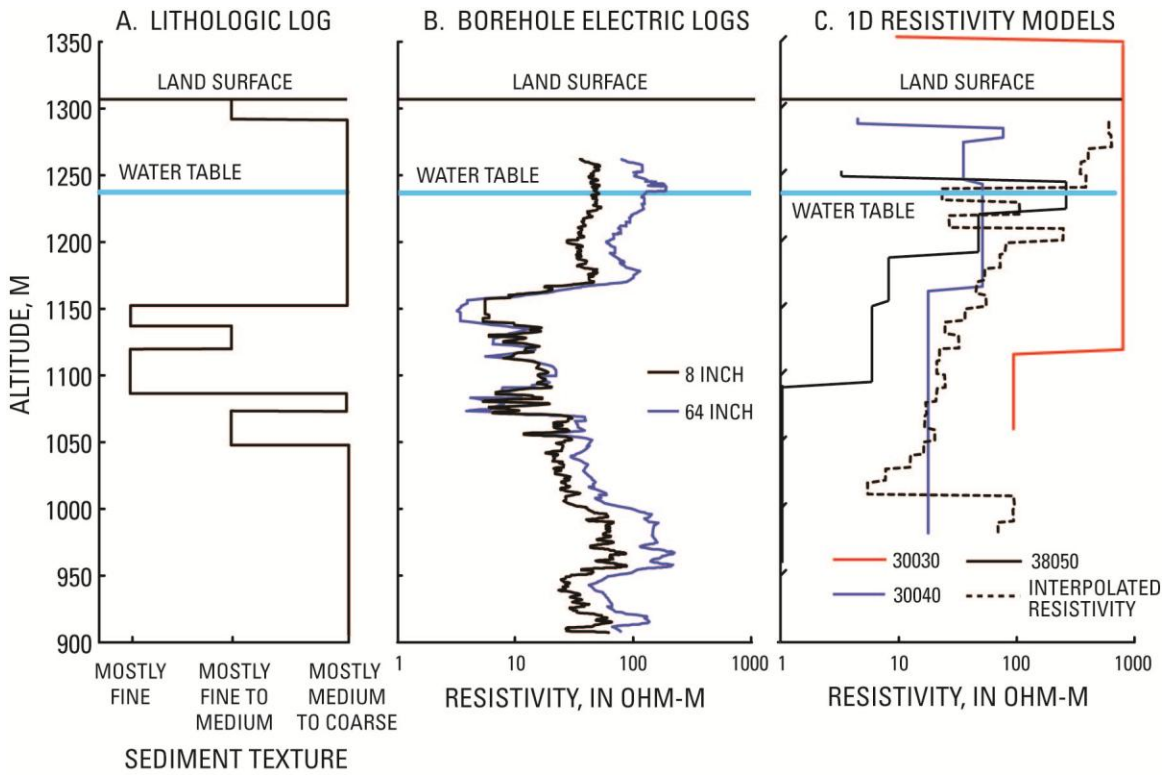

Figure 4 Comparison between resistivity logs, interpolated output from 1D resistivity models along nearby GEOTEM flight lines, and sediment texture from lithologic logs at well D-17-30 31AAB.

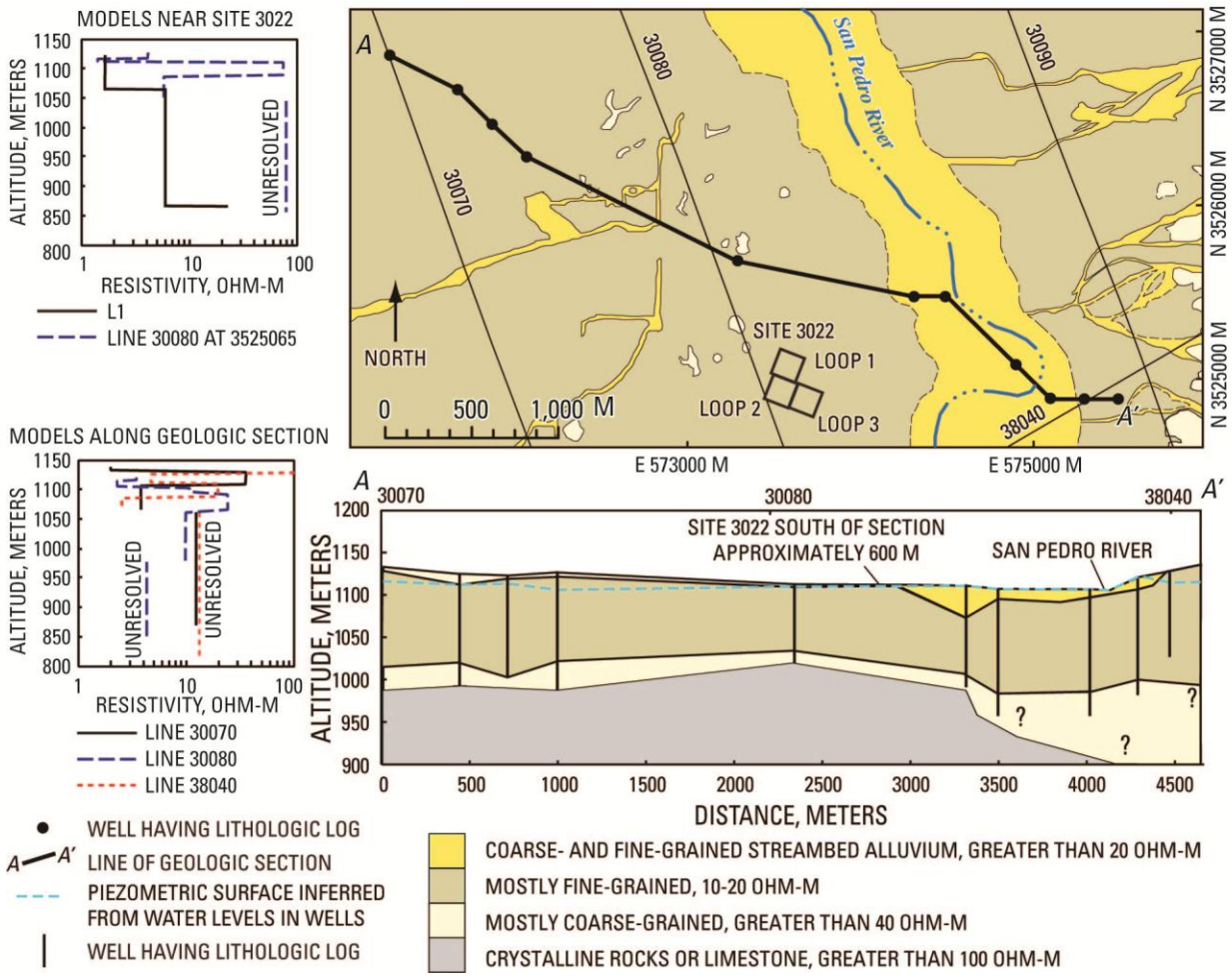

Figure 5 Geologic section A–A' and 1D models of airborne and ground TEM data near site 3022. The upper 100 m of the models indicate conductive sediments described by lithologic logs along the section. Below 100 m, mostly coarse-grained sediments are unresolved by the lowest model layers. Geology modified from Cook et al. (2009).

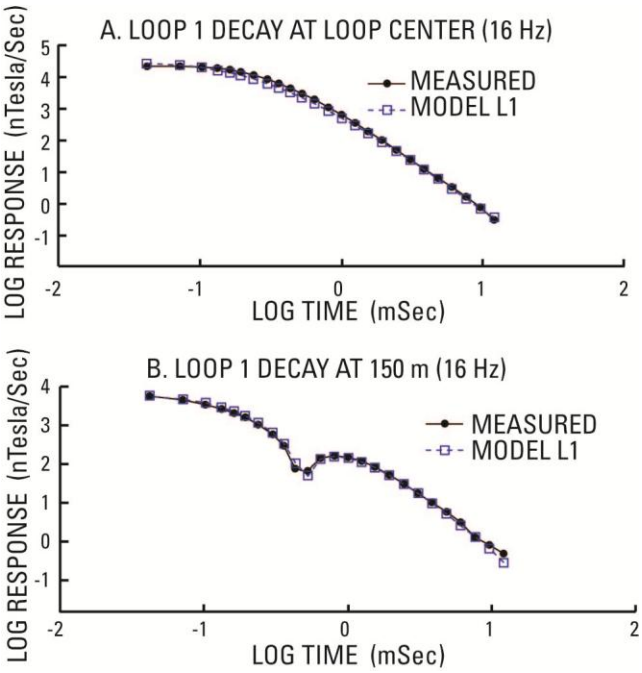

Figure 6 Fit of Model L1 (blue) to the ground data (black) for Loop 1 at site 3022 a) inside the loop and b) outside the loop (150 m).

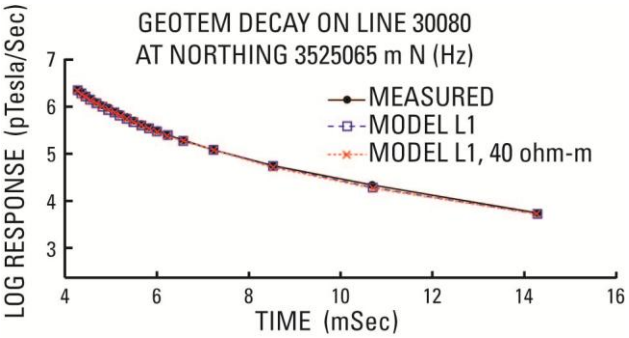

Figure 7 Fit of Model L1 (blue) to the airborne data (black) at 3525065 on Line 30080. In red is the response of Model L1 with the bottom three layers replaced with a single 40 ohm-m layer.

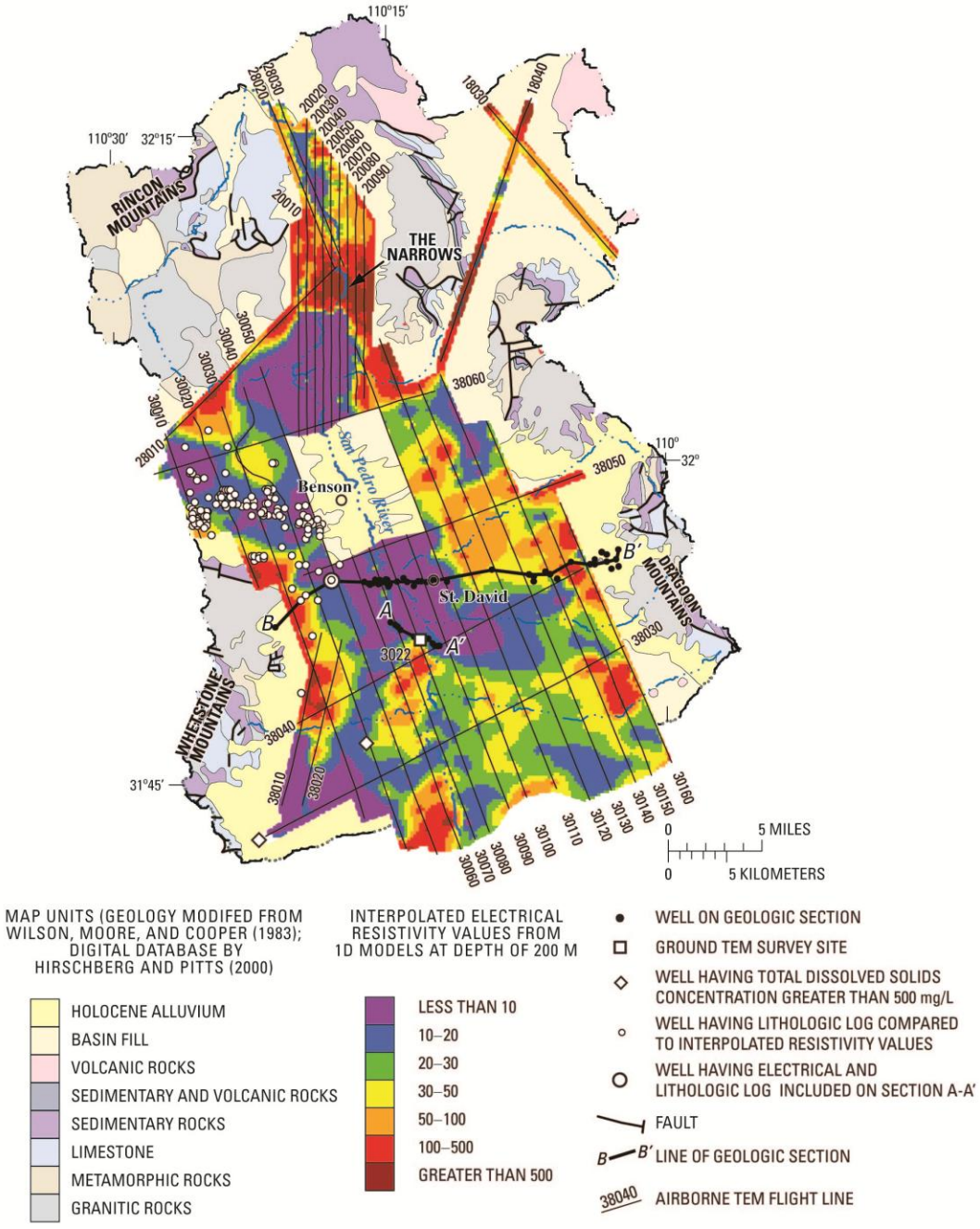

Figure 8 Interpolated resistivity values from 1D resistivity models at a depth of 200 m. The interpolation extent is limited to the horizontal area having output from the resistivity models within the altitude range. This omits an area of nearly 100 km^2 area surrounding the town of Benson. High salinity may contribute to low resistivity values in the southwest portion of the surveyed region. Lithologic descriptions from drill logs at 166 boreholes, shown as small white circles, are used to evaluate interpolated resistivity values.

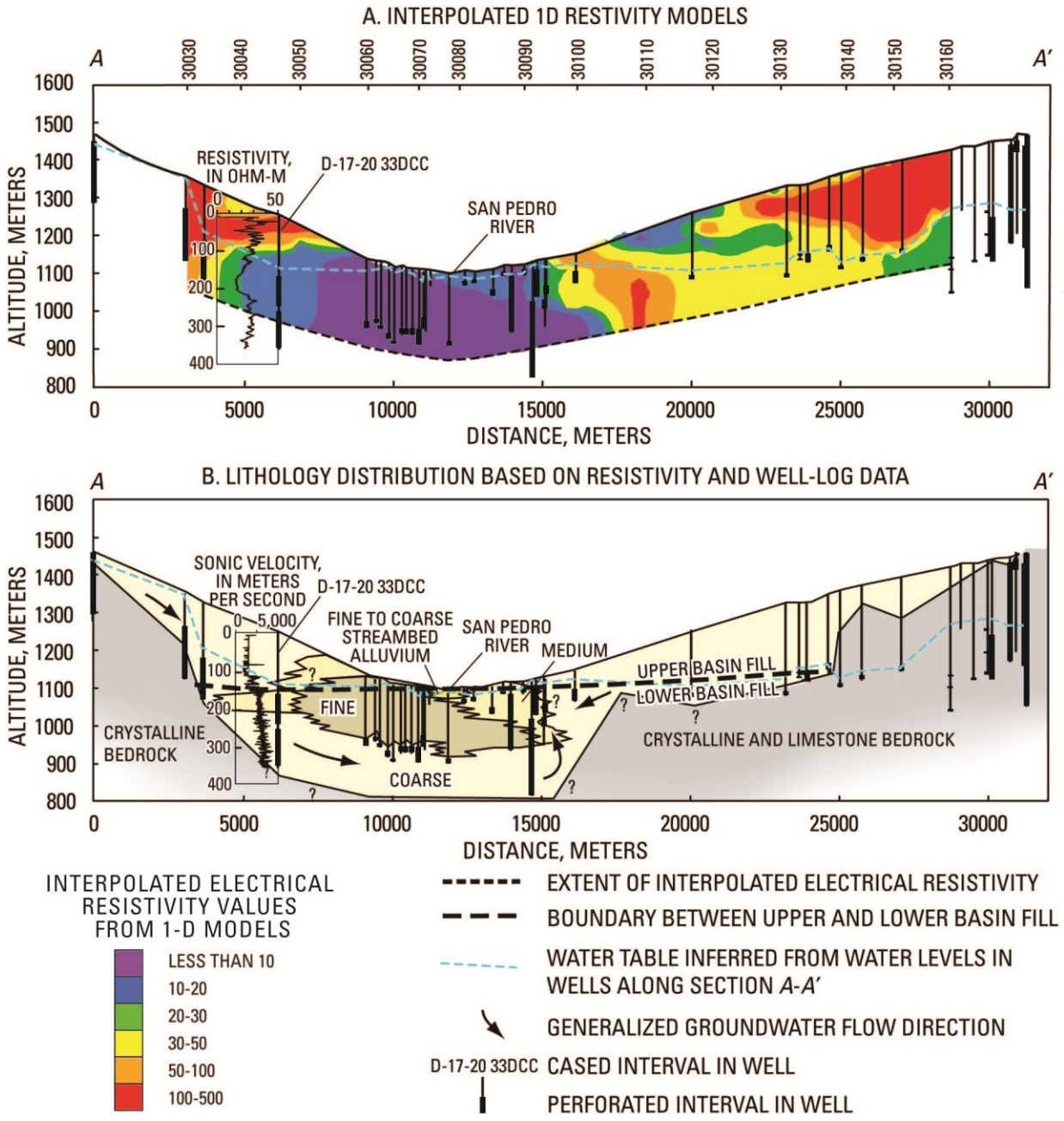

Figure 9 Distributions of (A) resistivity and (B) inferred lithology from the interpolated 1D resistivity models, resistivity log, and lithologic logs along section B–B'. The sonic log identified denser sediments of lower basin fill. Fine-grained sediments at the basin center are expected to be less permeable than underlying coarse-grained sediments. On the basis of inferred lithology distribution, groundwater generally flows from areas of higher water-table elevation near the basin margins in unconfined conditions, and toward the basin center under semi-confined conditions in areas of thick fine-grained sediments at the basin center.

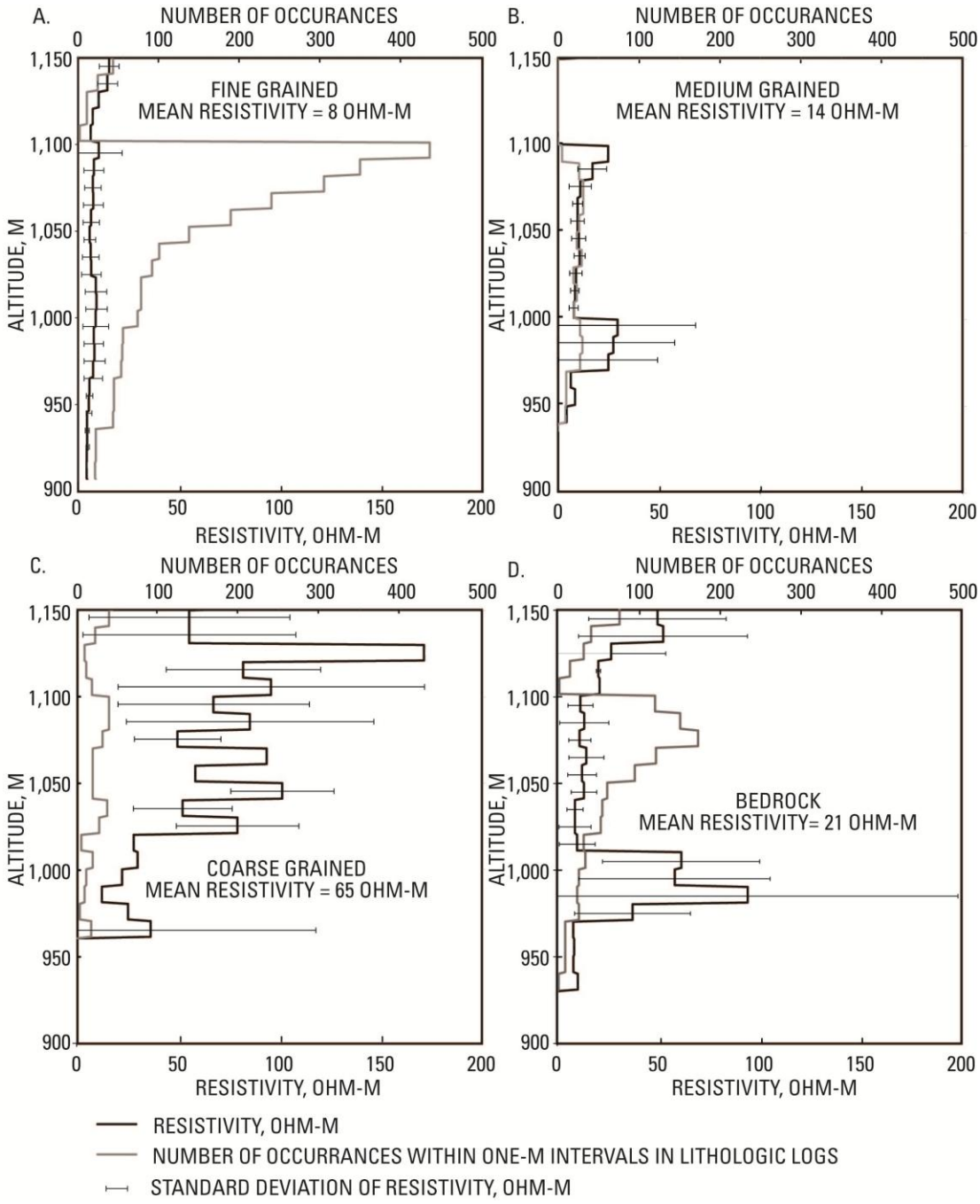

Figure 10 Comparison of interpolated resistivity values and lithology from saturated intervals in drill logs at wells near the city of Benson. Resistivity values average 8 ohm-m for fine-grained sediments (A), 14 ohm-m for medium-grained sediments (B), and 65 ohm for coarse-grained sediments (C). Bedrock lithology (D) includes pre-basin fine-grained mudstone and granite, which results in a wide range of resistivity values from about 5 ohm-m to 100 ohm.

LIST OF TABLES

Hydrogeologic Unit	Lithologic description	Saturated resistivity, ohm-m	Sonic velocity, m/s
Stream alluvium	Sand and gravel	10–50	500–1,500
Upper Basin Fill	Clay, silt, sand, and gravel	10–100	1,500–2,000
Lower Basin Fill	silt, sand, and gravel	Silt and clay less than 10–30	Silt and clay 1,500–2,000
		Sand and gravel 30–70	Sand and gravel 2,000–5,000
Tertiary and Cretaceous pre-basin sediments	Siltstone and conglomerate	10–30	3,000–5,000
Crystalline and limestone bedrock	Granite and limestone	Often greater than 100	3,000–5,000

Table 1.

References

Anderson, T. W., Geoffrey W. Freethey, and Patrick Tucci. 1992. Geohydrology and Water Resources of Alluvial Basins in South-Central Arizona and Parts of Adjacent States. In *U.S. Geological Survey Professional Paper*: U.S. Geological Survey.

Annan, A. P., and R. Lockwood. 1991. An application of airborne GEOTEM* in Australian conditions. *Exploration Geophysics* 22 (1):5-12.

Auken, Esben, Flemming Jørgensen, and Kurt I. Sørensen. 2003. Large-scale TEM investigation for groundwater. *Exploration Geophysics* 34:188-194.

Auken, Esben, Louise Pellerin, Niels B. Christensen, and Kurt Sorensen. 2006. A survey of current trends in near-surface electrical and electromagnetic methods. *Geophysics* 71 (5):G249-G260.

Baldridge, W. Scott, Gregory L. Cole, Bruce A. Robinson, and George R. Jiracek. 2007. Application of time-domain airborne electromagnetic induction to hydrogeologic investigations on the Pajarito Plateau, New Mexico, USA. *Geophysics* 72 (2):B31-B45.

Coes, Alissa L., D. J. Gellenbeck, and Douglas Clark Towne. 1999. *Ground-water quality in the Sierra Vista subbasin, Arizona, 1996-97*: U.S. Geological Survey Water-Resources Investigations Report 99-4056.

Cook, Joseph P., Ann Youberg, Phillip A. Pearthree, Jill A. Onken, Bryan J. MacFarlane, David E. Haddad, Erica R. Bigio, and Andrew L. Kowler. 2009. Mapping of Holocene river alluvium along the San Pedro River, Aravaipa Creek, ,and Babocamari River, southeastern Arizona. In *Digital Map RM-1*: Arizona Geological Survey.

d'Ozouville, Noémi, Esben Auken, Kurt Sorensen, Sophie Violette, Ghislain de Marsily, Benoit Deffontaines, and Godfrey Merlen. 2008. Extensive perched aquifer and structural implications revealed by 3D resistivity mapping in a Galapagos volcano. *Earth and Planetary Science Letters* 269 (3-4):518-522.

Danielsen, Jens E., Esben Auken, Flemming Jørgensen, Verner Søndergaard, and Kurt I. Sørensen. 2003. The application of the transient electromagnetic method in hydrogeophysical surveys. *Journal of Applied Geophysics* 53 (4):181-198.

Dickinson, William. R. 1991. *Tectonic setting of faulted Tertiary strata associated with the Catalina core complex in southern Arizona*, *Special Paper 264*. Boulder, CO: Geological Society of America.

Eberly, L. D., and T. B. Stanley. 1978. Cenozoic stratigraphy and geologic history of southwestern Arizona. *Geol Soc Am Bull* 89 (6):921-940.

Errol L. Montgomery & Associates, Inc. 2006. Results of drilling, construction, and testing at three groundwater exploration sites, Whetstone Ranch, Cochise County, Arizona. Tucson, AZ.

Fitterman, David V. 1987. Examples of transient sounding for ground-water exploration in sedimentary aquifers. *Ground Water* 25 (6):685-692.

Fitterman, David V., and Maryla Deszcz-Pan. 2001. Saltwater Intrusion in Everglades National Park, Florida Measured by Airborne

Electromagnetic Surveys. Paper read at First International Conference on Saltwater Intrusion and Coastal Aquifers: Monitoring, Modeling, and Management, April 23—25, 2001, at Essaouira, Morocco.

Fitterman, David V., Christopher M. Menges, Abdullah M. Al Kamali, and Fuad Essa Jama. 1991. Electromagnetic mapping of buried paleochannels in eastern Abu Dhabi Emirate, U.A.E. *Geoexploration* 27 (1-2):111-133.

Fitterman, David V., and Mark T. Stewart. 1986. Transient electromagnetic sounding for groundwater. *Geophysics* 51 (4):995-1005.

Fleming, John B., and D. R. Pool. 2002. Electrical Surveys to Define Distributions of Silt and Clay Layers Near the San Pedro River, Sierra Vista Subwatershed of the Upper San Pedro River Basin. Paper read at Symposium on the Application of Geophysics to Environmental and Engineering Problems, at Las Vegas, Nevada, February 2002.

Gabriel, Gerald, Reinhard Kirsch, Bernhard Siemon, and Helga Wiederhold. 2003. Geophysical investigation of buried Pleistocene subglacial valleys in Northern Germany. *Journal of Applied Geophysics* 53 (4):159-180.

Hereford, Richard. 1993. Entrenchment and widening of the Upper San Pedro River, Arizona. In *Geological Society of America Special Paper 282*: Geological Society of America.

Jørgensen, Flemming, Peter B. E. Sandersen, and Esben Auken. 2003. Imaging buried Quaternary valleys using the transient electromagnetic method. *Journal of Applied Geophysics* 53 (4):199-213.

Jørgensen, Flemming, Peter B.E. Sandersen, Esben Auken, Holger Lykke-Andersen, and Kurt Sørensen. 2005. Contributions to the geological mapping of Mors, Denmark – A study based on a large-scale TEM survey. *Bulletin of the Geological Society of Denmark* 52:53-75.

EMIGMA 7.8. Petros Eikon, Inc., Concord, ON.

Pool, D. R., and Alissa L. Coes. 1999. Hydrogeologic investigations of the Sierra Vista subwatershed of the upper San Pedro Basin, Cochise County, southeast Arizona: U.S. Geological Survey Water-resources Investigations Report 99-4197.

Pool, D. R., and Jesse E. Dickinson. 2007. Ground-water flow model of the Sierra Vista subwatershed and Sonoran portions of the upper San Pedro basin, southeastern Arizona, United States, and northern Sonora, Mexico. Reston, Va.: U.S. Geological Survey Scientific Investigations Report 2006-5228.

Robinson, D. A., A. Binley, N. Crook, F. D. Day-Lewis, T. P. A. Ferre, V. J. S. Grauch, R. Knight, M. Knoll, V. Lakshmi, R. Miller, J. Nyquist, L. Pellerin, K. Singha, and L. Slater. 2008. Advancing process-based watershed hydrological research using near-surface geophysics: a vision for, and review of, electrical and magnetic geophysical methods. *Hydrological Processes* 22:3604-3635.

Rodriguez, Brian D., Maryla Deszcz-Pan, V. J. S. Grauch, Jon P. Doucette, and David A. Sawyer. 2001. Mapping Grain Size Facies for the Hydrogeologic Model of the Middle Rio Grande Basin, New Mexico Using Airborne Time-Domain Electromagnetic Data. In *Symposium on the Application of Geophysics to Engineering & Environmental Problems*.

Scarborough, R. B., and H. W. Peirce. 1978. Late Cenozoic basins of Arizona. In *Land of Cochise, Southeastern Arizona, New Mexico Geological Society Guidebook, 29th field conference*, edited by J. F. Callender, J. C. Wilt and R. E. Clemons.

Shafiqullah, M., P.E. Damon, D.J. Lynch, S.J. Reynolds, W.A. Rehrig, and R.H. Raymond. 1980. K–Ar geochronology and geologic history of southwestern Arizona and adjacent areas. In *Studies in Western Arizona*, edited by J. P. Jenny and C. Stone. Tucson, AZ: Arizona Geological Society Digest.

Smith, Richard S., Michael D. O'Connell, and Lene Hjelm Poulsen. 2004. Using airborne electromagnetics surveys to investigate

the hydrogeology of an area near Nyborg, Denmark. *Near Surface Geophysics*:123-130.

Telford, W. M., L. P. Geldart, R. E. Sheriff, and D. A. Keys. 1976. *Applied geophysics*. London: Cambridge University Press.

Wynn, Jeff. 2006. Mapping Ground Water in Three Dimensions - An Analysis of Airborne Geophysical Surveys of the Upper San Pedro River Basin, Cochise County, Southeastern Arizona: U.S. Geological Survey Professional Paper 1674.

Zohdy, Adel A. R., Gordon P. Eaton, and Don R. Mabey. 1974. *Application of surface geophysics to ground-water investigations*, *Techniques of water-resources investigations of the United States Geological Survey*. Washington: U.S. Dept. of the Interior, Geological Survey : U.S. Govt. Print. Off.